Advances in Applied Mathematics and Mechanics
Adv. Appl. Math. Mech., Vol. **9**, No. 6, pp. 1485-1505

DOI: 10.4208/aamm.OA-2016-0121
December 2017

Nonlinear Vibrations of Two-Span Composite Laminated Plates with Equal and Unequal Subspan Lengths

Lingchang Meng and Fengming Li*

College of Mechanical Engineering, Beijing University of Technology, Beijing 100124, China

Received 17 September 2016; Accepted (in revised version) 23 February 2017

Abstract. The nonlinear transverse vibrations of ordered and disordered two-dimensional (2D) two-span composite laminated plates are studied. Based on the von Karman's large deformation theory, the equations of motion of each-span composite laminated plate are formulated using Hamilton's principle, and the partial differential equations are discretized into nonlinear ordinary ones through the Galerkin's method. The primary resonance and 1/3 sub-harmonic resonance are investigated by using the method of multiple scales. The amplitude-frequency relations of the steady-state responses and their stability analyses in each kind of resonance are carried out. The effects of the disorder ratio and ply angle on the two different resonances are analyzed. From the numerical results, it can be concluded that disorder in the length of the two-span 2D composite laminated plate will cause the nonlinear vibration localization phenomenon, and with the increase of the disorder ratio, the vibration localization phenomenon will become more obvious. Moreover, the amplitude-frequency curves for both primary resonance and 1/3 sub-harmonic resonance obtained by the present analytical method are compared with those by the numerical integration, and satisfactory precision can be obtained for engineering applications and the results certify the correctness of the present approximately analytical solutions.

AMS subject classifications: 70-08, 35Q72, 65M60

Key words: Ordered and disordered two-span composite laminated plates, nonlinear vibration localization, method of multiple scales, primary and 1/3 sub-harmonic resonances.

1 Introduction

Multi-span structures are important structural elements that are widely used in various

*Corresponding author.
Email: fmli@bjut.edu.cn (F. M. Li)

engineering applications such as aeroplane panels, slabs in house construction, glass window panels and bridge decks. Vibration of multi-span beams and plates with internal line supports have been an intensive research focus from many researchers for several decades. However, most of them focused on the analysis of natural frequencies of free linear vibration, and the numerical approximate solutions or Levy solutions of free or forced linear vibration.

Veletsos and Newmark [1] calculated the natural frequencies of plates with internal line supports in one direction by employing the Holzer's method. Abramovich et al. [2] carried out the analysis on the vibration frequencies of multi-span non-symmetric composite beams using the exact element method considering the effects of rotary inertia and shear deformations and gave the mode shapes for the clamped-clamped boundary conditions. Wang and Lin [3] proposed the component method to study the free vibration of a multi-span Mindlin plate to a moving load and analyzed the orthogonality of any two distinct sets of the mode shape functions. They discussed the effects of span number, rotary inertia and transverse shear deformation on the critical velocity of the plates. Wang [4] investigated the effects of span member, rotary inertia and shear deformation on the maximum moment, maximum deflection and critical velocity of multi-span Timoshenko beams using the method of modal analysis.

Xiang and Wei [5] presented the exact solution for the vibration of multi-span rectangular Mindlin plates and obtained the exact vibration frequencies varying with the span ratios, number of spans and boundary conditions. Zhao et al. [6] introduced discrete singular convolution to solve the vibration of plates under complex and irregular internal support conditions. Xiang et al. [7] presented a Levy solution to investigate the vibration behavior of multi-span rectangular plates and studied the impact of the internal line supports on the vibration behavior by varying both the number of internal line supports and support positions. Xiang and Reddy [8] employed the levy type solution, state-space technique and first order shear deformation plate theory to study the natural vibration of rectangular plate with an internal line hinge. Lv et al. [9] investigated the influence of location of internal line supports on the natural frequencies of multi-span plates with large aspect ratios based on the classical Kirchhoff plate theory.

Mikata [10] mathematically proved the orthogonality condition of the eigenfunctions for multi-span beams of variable cross-section and obtained an exact closed-form solution as an application of the general orthogonality condition. Song and Li [11] investigated the influences of the disorder degree on the vibration localization and aeroelastic properties of the two-span panels in supersonic airflow. Li and Song [12] studied the vibration properties of nearly periodic two-span beams and used the velocity feedback control algorithm to design the active controller.

The nonlinear vibration characteristics in various engineering structures have also attracted numerous researchers' attention. Özkaya et al. [13, 14] investigated the nonlinear transverse vibrations and 3:1 internal resonance of a beam or a tensional beam on multiple supports applying the method of multiple scales. Davtabal et al. [15] constructed an electromechanical device to investigate the frequency-dependent vibrations of a

multi-span beam made of two parallel rods, and presented the experimental time histories, phase planes and bifurcation diagrams to illustrate richness of the system dynamics. Lewandowski [16] studied nonlinear free vibrations of multi-span beams on elastic supports using the dynamic finite element method and determined the frequencies and nonlinear vibration modes. Eftekhari and Jafari [17] proposed a mixed method that combined the finite element method, differential quadrature method, and integral quadrature method to study the forced vibration of multi-span rectangular plates carrying moving masses. Tubaldi et al. [18, 19] investigated the geometrically non-linear vibrations and stability of a periodically supported rectangular plate subjected to axial flow.

Shen et al. [20–22] studied the nonlinear dynamical problems of the Duffing oscillator of fractional-order derivatives using the multiple scales method, incremental harmonic balance method and averaging method. Rostami and Haeri [23] took advantage of the describing function method to estimate the frequency and the amplitude of a fractional-order Duffing oscillator. Gao and Yu [24] numerically studied the chaotic behaviors in the fractional-order symmetric and non-symmetric periodically forced Duffing's oscillators. Ge and Ou [25] numerically studied the chaotic behaviors in a fractional order modified Duffing system through the phase portraits, Poincaré maps and bifurcation diagrams.

Li and Yao [26] investigated the effects of subsonic air flow and ply angles on the 1/3 sub-harmonic resonance of a nonlinear composite laminated cylindrical shell. Abdelhafez [27] analyzed certain forms of resonances of a vibratory system with quadratic, cubic and quartic nonlinearities subjected to a sinusoidal excitation and compared the analytical solutions with the numerical ones. Younesian and Nououzi [28] researched the primary, super-harmonic and sub-harmonic resonances of a nonlinear viscoelastic plate subjected to subsonic flow and external excitation. Amabili et al. [29–31] systematically studied the nonlinear vibrations of rectangular plates from both the theoretical and experimental methods.

Although many investigations on the vibrations of multi-span structures have been conducted, up to now, few results on the nonlinear vibration properties of ordered and disordered two-span composite laminated plates have been reported, which motivates us to carry out the present study. The aim of this paper is to focus on the nonlinear transverse vibrations of two-span composite laminated plates with equal (ordered) and unequal (disordered) subspan lengths. The geometrical nonlinearity of the structure is taken into account. The equation of motion of the structure is obtained by Hamilton's principle and reduced into a nonlinear ordinary differential equation using the Galerkin's method. The primary and 1/3 sub-harmonic resonances of the ordered and disordered two-span composite laminated plate are analyzed by means of the method of multiple scales. The effects of the disorder ratio and ply angle on the nonlinear resonances and vibration localization phenomenon are discussed. Moreover, comparisons of the amplitude frequency curves obtained by the present analytical solutions and those of numerical integration scheme are fulfilled to certify the correctness and satisfactory precision of the present approximate analytical method.

2 Equation of motion

Fig. 1 shows the two-dimensional (2D) two-span composite laminated plate composed of n layers. The plate is subjected to an uniform harmonic external excitation $F\cos(\Omega t)$ and in-plane compression force N. The local coordinate system is also displayed in Fig. 1, in which the positive direction of the x-axis for the left span is to the right and the positive direction for the right span is to the left, and the x-axis of this coordinate system locates at the mid-plane of the plate. The total uniform thickness, total length, and lengths of the left and right span are h, l, l_1 and l_2, respectively. The displacement of the internal line support with respect to the symmetric location of the plate is denoted by Δl and $v=2\Delta l/l$ is defined as the disorder ratio.

Kirchhoff Laminated Plate Theory is applied in the structural modeling. According to the von Karman's large deflection theory, the strain-displacement relations for each span of the plate are

$$\varepsilon_{x_i}=-z\frac{\partial^2 w_i}{\partial {x_i}^2}+\frac{1}{2}\left(\frac{\partial w_i}{\partial x_i}\right)^2, \quad i=1,2, \tag{2.1}$$

where w_1 and w_2 are the transverse displacements of the left and right span plates.

For orthotropic material, the stress-strain relation for the k-th layer is expressed as

$$\begin{Bmatrix}\sigma_1\\ \sigma_2\\ \tau_{12}\end{Bmatrix}=\begin{bmatrix}Q_{11} & Q_{12} & 0\\ Q_{12} & Q_{22} & 0\\ 0 & 0 & Q_{66}\end{bmatrix}\begin{Bmatrix}\varepsilon_1\\ \varepsilon_2\\ \gamma_{12}\end{Bmatrix}=Q\begin{Bmatrix}\varepsilon_1\\ \varepsilon_2\\ \gamma_{12}\end{Bmatrix}, \tag{2.2}$$

where σ_1, σ_2 and τ_{12} are the normal and shear stresses, ε_1, ε_2 and γ_{12} are the normal and shear strains in the 1-2 (principal directional) plane, $Q_{11}=E_{11}/(1-v_{12}v_{21})$, $Q_{12}=v_{12}E_{22}/(1-v_{12}v_{21})$, $Q_{22}=E_{22}/(1-v_{12}v_{21})$ and $Q_{66}=G_{12}$ are the stiffness coefficients, where E_{11}, E_{22} and G_{12} are the elastic and shear moduli, and v_{12} and v_{21} are the Poisson's ratios.

The transformed stress-strain relation of the k-th layer of the laminated plate with ply angle θ_k in the Cartesian coordinates is [32,33]

$$\sigma_{x_i}^k=\bar{Q}_{11}^k\varepsilon_{x_i}, \tag{2.3}$$

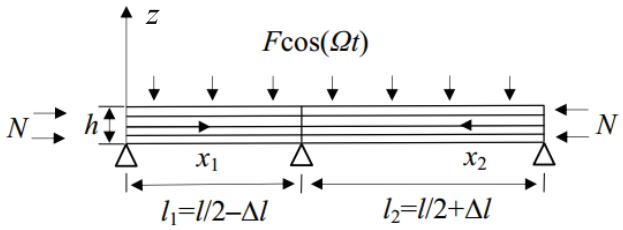

Figure 1: Schematic diagram of a two-span composite laminated plate.

where

$$\bar{Q}_{11}^k = Q_{11}\cos^4\theta_k + 2(Q_{12}+2Q_{66})\sin^2\theta_k\cos^2\theta_k + Q_{22}\sin^4\theta_k$$

is the transformed stiffness.

The strain energy of each span of the plate can be written as

$$\begin{aligned} U_i &= \frac{1}{2}\sum_{k=1}^{n}\int_0^{l_i}\int_{z_{k-1}}^{z_k}\sigma_{x_i}^k\varepsilon_{x_i}dx_i dz - \frac{1}{2}\int_0^{l_i}N\Big(\frac{\partial w_i}{\partial x_i}\Big)^2 dx_i \\ &= \frac{1}{2}\int_0^{l_i}\Big[\frac{1}{4}A_{11}\Big(\frac{\partial w_i}{\partial x_i}\Big)^4 + D_{11}\Big(\frac{\partial^2 w_i}{\partial x_i^2}\Big)^2\Big]dx_i - \frac{1}{2}\int_0^{l_i}N\Big(\frac{\partial w_i}{\partial x_i}\Big)^2 dx_i, \quad i=1,2, \end{aligned} \tag{2.4}$$

where z_{k-1} and z_k are the vertical coordinates of the lower and upper surfaces of the k-th layer, and

$$A_{11} = \sum_{k=1}^{n}\bar{Q}_{11}^k(z_k - z_{k-1}) \quad \text{and} \quad D_{11} = \frac{1}{3}\sum_{k=1}^{n}\bar{Q}_{11}^k(z_k^3 - z_{k-1}^3).$$

The kinetic energy of each span of the plate is

$$T_i = \frac{1}{2}\int_0^{l_i}\rho h\Big(\frac{\partial w_i}{\partial t}\Big)^2 dx_i, \quad i=1,2, \tag{2.5}$$

where ρ is the mass density of the composite laminated plate.

The virtual work of the external forces, δW_i can be expressed as

$$\delta W_i = \int_0^{l_i}\Big[F\cos(\Omega t) - c\frac{\partial w_i}{\partial t}\Big]\delta w_i dx_i, \tag{2.6}$$

where c is the structural damping coefficient.

Substituting Eqs. (2.4), (2.5) and (2.6) into the following Hamilton's principle [32]:

$$\int_{t_1}^{t_2}\delta(T_i - U_i)dt + \int_{t_1}^{t_2}\delta W_i dt = 0, \tag{2.7}$$

and performing the variation operation in terms of w_i, one can obtain the nonlinear partial differential equation of motion for each span of the composite laminated plate

$$\rho h\frac{\partial^2 w_i}{\partial t^2} + D_{11}\frac{\partial^4 w_i}{\partial x_i^4} + \Big[N - \frac{3}{2}A_{11}\Big(\frac{\partial w_i}{\partial x_i}\Big)^2\Big]\frac{\partial^2 w_i}{\partial x_i^2} + c\frac{\partial w_i}{\partial t} = F\cos(\Omega t), \quad i=1,2. \tag{2.8}$$

In order to study the nonlinear vibration behaviors of the two-span composite laminated plate, the transverse displacement of each span of the plate can be expressed as

$$w_i(x_i,t) = W_i(x_i)Q_i(t), \quad i=1,2, \tag{2.9}$$

where $W_i(x_i)$ is the mode shape and $Q_i(t)$ is the generalized coordinate.

For the simply supported two-span plate with internal rigid line support, the boundary conditions are given by

$$w_1(0,t)=0, \quad \frac{\partial^2 w_1(0,t)}{\partial x_1^2}=0, \tag{2.10a}$$

$$w_1(l_1,t)=0, \quad w_2(l_2,t)=0, \quad \frac{\partial w_1(l_1,t)}{\partial x_1}=-\frac{\partial w_2(l_2,t)}{\partial x_2}, \quad \frac{\partial^2 w_1(l_1,t)}{\partial x_1^2}=\frac{\partial^2 w_2(l_2,t)}{\partial x_2^2}, \tag{2.10b}$$

$$w_2(0,t)=0, \quad \frac{\partial^2 w_2(0,t)}{\partial x_2^2}=0. \tag{2.10c}$$

For the vibration analysis, the expressions of the mode shape $W_i(x_i)$ should be presented. By means of the modal analysis method in [10,12] and based on the boundary conditions in Eq. (2.10), the mode shapes of the two-span structure can be expressed as:

$$W_i(x_i)=A_i\sin(\beta x_i)+B_i\cos(\beta x_i)+C_i\sinh(\beta x_i)+D_i\cosh(\beta x_i), \tag{2.11}$$

where $\beta^4=\varpi^2\rho h/D_{11}$, ϖ is the natural frequency which can be determined by the following characteristic equation, and A_i, B_i, C_i, D_i are the undetermined coefficients.

Substituting Eqs. (2.9) and (2.11) into Eqs. (2.10a) and (2.10c), the following equation can be obtained

$$B_i+D_i=0, \quad -B_i+D_i=0. \tag{2.12}$$

By solving Eq. (2.12), one can obtain $B_i=D_i=0$, and thus the expression of the mode shape in Eq. (2.11) can be simplified. Substitution of Eq. (2.9) and the simplified mode shape into Eq. (2.10b) leads to the following equations

$$A_1\sin(\beta l_1)+C_1\sinh(\beta l_1)=0, \tag{2.13a}$$

$$A_2\sin(\beta l_2)+C_2\sinh(\beta l_2)=0, \tag{2.13b}$$

$$A_1\cos(\beta l_1)+C_1\cosh(\beta l_1)+A_2\cos(\beta l_2)+C_2\cosh(\beta l_2)=0, \tag{2.13c}$$

$$-A_1\sin(\beta l_1)+C_1\sinh(\beta l_1)+A_2\sin(\beta l_2)-C_2\cosh(\beta l_2)=0. \tag{2.13d}$$

Existing of non-trivial solutions of Eq. (2.13) requires its coefficient determinant to be zero, from which the characteristic equation of the two-span structure can be obtained:

$$\begin{aligned}&\sin(\beta l_1)\sin(\beta l_2)[\cosh(\beta l_1)\sinh(\beta l_2)+\sinh(\beta l_1)\cosh(\beta l_2)]\\&-\sinh(\beta l_1)\sinh(\beta l_2)[\cos(\beta l_1)\sin(\beta l_2)+\sin(\beta l_1)\cos(\beta l_2)]=0.\end{aligned} \tag{2.14}$$

And one of the non-trivial solutions of Eq. (2.13) can be calculated as:

$$A_1=-\sinh(\beta l_1), \qquad C_1=\sin(\beta l_1), \tag{2.15a}$$

$$A_2=-\frac{\sin(\beta l_1)\sinh(\beta l_1)}{\sin(\beta l_2)}, \qquad C_2(x_2)=\frac{\sin(\beta l_1)\sinh(\beta l_1)}{\sinh(\beta l_2)}. \tag{2.15b}$$

Thus the expressions of the mode shapes of the two-span structure can be expressed as

$$W_1(x_1) = -\sinh(\beta l_1)\sin(\beta x_1) + \sin(\beta l_1)\sinh(\beta x_1), \tag{2.16a}$$

$$W_2(x_2) = -\frac{\sin(\beta l_1)\sinh(\beta l_1)}{\sin(\beta l_2)}\sin(\beta x_2) + \frac{\sin(\beta l_1)\sinh(\beta l_1)}{\sinh(\beta l_2)}\sinh(\beta x_2). \tag{2.16b}$$

Introducing the following dimensionless parameters:

$$q_i = \frac{l}{h^2}Q_i, \quad (i=1,2), \quad \bar{t} = t\sqrt{\frac{D_{11}}{\rho h l^4}}, \quad R_x = \frac{l^2 N}{D_{11}}, \tag{2.17a}$$

$$R = \frac{-3h^4 A_{11}}{2l^2 D_{11}}, \quad \lambda = \frac{cl^2}{\sqrt{\rho h D_{11}}}, \quad \Delta p = \frac{l^5 F}{h^2 D_{11}}, \quad \omega' = \Omega\sqrt{\frac{\rho h l^4}{D_{11}}}. \tag{2.17b}$$

Substituting Eqs. (2.9) and (2.17) into Eq. (2.8) and applying the Galerkin's method, the following dimensionless nonlinear ordinary equations in terms of the generalized coordinate $q_i(\bar{t})$ can be obtained:

$$M_i\ddot{q}_i(\bar{t}) + C_i\dot{q}_i(\bar{t}) + K_i q_i(\bar{t}) + \Theta_i q_i^3(\bar{t}) = F_i\cos(\omega'\bar{t}), \quad (i=1,2), \tag{2.18}$$

where the coefficients are written as:

$$M_i = \int_0^{l_i} W_i^2 dx_i, \quad C_i = \lambda M_i, \quad K_i = \int_0^{l_i} \frac{d^4 W_i}{\partial x_i^4} W_i dx_i + R_x \int_0^{l_i} \frac{d^2 W_i}{\partial x_i^2} W_i dx_i, \tag{2.19a}$$

$$\Theta_i = R\int_0^{l_i} \left(\frac{dW_i}{dx_i}\right)^2 \frac{d^2 W_i}{\partial x_i^2} W_i dx_i, \quad F_i = \Delta p \int_0^{l_i} W_i dx_i, \quad (i=1,2). \tag{2.19b}$$

3 Nonlinear vibration analyses of two-span composite laminated plates

3.1 Primary resonance analysis

For convenience of further analysis, introducing the variables $\tau = \bar{t}\sqrt{K_i/M_i}$, $\varepsilon\mu_i = C_i/2\sqrt{M_i K_i}$, $\varepsilon r_i = \Theta_i/K_i$, $\varepsilon f_i = F_i/K_i$, $\omega = \omega'\sqrt{M_i/K_i}$, $\omega_0 = 1$, where ε is a small parameter, Eq. (2.18) is transformed into

$$\ddot{q}_i(\tau) + 2\varepsilon\mu_i\dot{q}_i(\tau) + \omega_0^2 q_i(\tau) + \varepsilon r_i q_i^3(\tau) = \varepsilon f_i\cos(\omega\tau), \quad (i=1,2). \tag{3.1}$$

In this section, the primary resonance case of $\omega \approx \omega_0$, i.e., $\omega = \omega_0 + \varepsilon\sigma$, where σ is the detuning parameter will be considered, and the study will be confined to the case of small damping, weak nonlinearity and soft excitation.

Assume that the solution of Eq. (3.1) can be represented by a two time scales expression in the form

$$q_i(t) = X_{i0}(T_0, T_1) + \varepsilon X_{i1}(T_0, T_1) + \cdots, \tag{3.2}$$

where $T_0=\tau$ and $T_1=\varepsilon\tau$ are the two time scales. Substituting Eq. (3.2) into Eq. (3.1), and equating the coefficients of ε^0 and ε^1, the following equations can be obtained:

$$D_0^2X_{i0}+X_{i0}=0, \tag{3.3a}$$

$$D_0^2X_{i1}+X_{i1}=-r_iX_{i0}^3-2D_0D_1X_{i0}-2\mu_iD_0X_{i0}+f_i\cos(\omega\tau). \tag{3.3b}$$

The solution of Eq. (3.3a) can be expressed as

$$X_{i0}(T_0,T_1)=A_i(T_1)e^{jT_0}+c.c., \tag{3.4}$$

where $c.c.$ denotes the complex conjugate of the preceding terms and $j^2=-1$. Substituting Eq. (3.4) into Eq. (3.3b) leads to

$$D_0^2X_{i1}+X_{i1}=-(2j\mu_iA_i+2jD_1A_i+3r_iA_i^2\bar{A}_i]e^{jT_0}-3r_iA_i^3e^{3jT_0}+\frac{f_i}{2}e^{jT_0}e^{j\sigma T_1}+c.c.. \tag{3.5}$$

The secular terms of Eq. (3.5) are eliminated by setting

$$2j\mu_iA_i+2jD_1A_i+3r_iA_i^2\bar{A}_i-\frac{f_i}{2}e^{j\sigma T_1}=0. \tag{3.6}$$

It is convenient to introduce the following notations:

$$A_i(T_1)=\frac{1}{2}a_i(T_1)e^{j\beta_i(T_1)}, \tag{3.7a}$$

$$\phi_i=T_1\sigma-\beta_i, \tag{3.7b}$$

where $a_i(T_1)$ and $\beta_i(T_1)$ are the real-valued functions of T_1. Substituting Eqs. (3.7a) and (3.7b) into Eq. (3.6) and separating the result into real and imaginary parts, one can obtain the differential equations of $a_i(T_1)$ and $\phi_i(T_1)$

$$D_1a_i=-\mu_ia_i-\frac{f_i}{2}\sin\phi_i, \tag{3.8a}$$

$$D_1\phi_i=\sigma-\frac{3r_ia_i^2}{8}+\frac{f_i}{2a_i}\cos\phi_i. \tag{3.8b}$$

By setting $D_1a_i=0$ and $D_1\phi_i=0$, the equations for amplitude $\bar{a}_i$ and phase $\bar{\phi}_i$ of the steady-state solutions of the primary resonance case can be obtained as

$$-\mu_i\bar{a}_i-\frac{f_i}{2}\sin\bar{\phi}_i=0, \tag{3.9a}$$

$$\sigma-\frac{3r_i\bar{a}_i^2}{8}+\frac{f_i}{2\bar{a}_i}\cos\bar{\phi}_i=0. \tag{3.9b}$$

Eliminating $\bar{\phi}_i$ from Eq. (3.9), one can get the amplitude-frequency equation of the primary resonance for each span of the plate

$$\mu_i^2+\left(\sigma-\frac{3r_i\bar{a}_i^2}{8}\right)^2=\left(\frac{f_i}{2\bar{a}_i}\right)^2,\quad (i=1,2). \tag{3.10}$$

To analyze the stability of the steady-state primary resonance, Eq. (3.8) is linearized at $(\bar{a}_i,\bar{\phi}_i)$ about the perturbation variables Δa_i and $\Delta\phi_i$,

$$D_1\Delta a_i=-\mu_i\Delta a_i+\frac{f_i}{2}\cos\bar{\phi}_i\Delta\phi_i, \tag{3.11a}$$

$$D_1\Delta\phi_i=-\Big(\frac{3r_i\bar{a}_i}{4}+\frac{f_i}{2\bar{a}_i^2}\cos\bar{\phi}_i\Big)\Delta a_i-\frac{f_i}{2\bar{a}_i}\sin\bar{\phi}_i\Delta\phi_i. \tag{3.11b}$$

According to Eq. (3.9), the characteristic equation of Eq. (3.11) can be expressed as

$$\begin{aligned}&\begin{vmatrix}\lambda_i+\mu_i & -\frac{f_i}{2}\cos\bar{\phi}_i\\ \frac{3r_i\bar{a}_i}{4}+\frac{f_i}{2\bar{a}_i^2}\cos\bar{\phi}_i & \lambda_i+\frac{f_i}{2\bar{a}_i}\sin\bar{\phi}_i\end{vmatrix}\\ &=\lambda_i^2+2\mu_i\lambda_i+\mu_i^2+\Big(\sigma-\frac{3r_i\bar{a}_i^2}{8}\Big)\Big(\sigma_i-\frac{9r_i\bar{a}_i^2}{8}\Big)=0.\end{aligned} \tag{3.12}$$

By means of the Routh-Hurwitz criterion [34], the steady-state vibration is asymptotically stable if and only if $\mu_i>0$ and $\mu_i^2+(\sigma-\frac{3r_i\bar{a}_i^2}{8})(\sigma-\frac{9r_i\bar{a}_i^2}{8})>0$.

3.2 1/3 Sub-harmonic resonance analysis

For convenience, introducing the variables $\tau=\bar{t}\sqrt{K_i/M_i}$, $\varepsilon\mu_i=C_i/2\sqrt{M_iK_i}$, $\varepsilon r_i=\Theta_i/K_i$, $G_i=F_i/K_i$, $\omega=\omega'\sqrt{M_i/K_i}$ and $\omega_0=1$, where ε is a small parameter, Eq. (2.18) is transformed into

$$\ddot{q}_i(\tau)+2\varepsilon\mu_i\dot{q}_i(\tau)+\omega_0^2q_i(\tau)+\varepsilon r_iq_i^3(\tau)=G_i\cos(\omega\tau). \tag{3.13}$$

In this section, the 1/3 sub-harmonic resonance case of $\omega\approx3\omega_0$, i.e., $\omega=3\omega_0+\varepsilon\sigma$ is considered, and the study is confined to the case of small damping and weak nonlinearity.

Substituting Eq. (3.2) into Eq. (3.13), and equating the coefficients of ε^0 and ε^1, we can obtain the following equations:

$$D_0^2X_{i0}+X_{i0}-G_i\cos(\omega\tau)=0, \tag{3.14a}$$

$$D_0^2X_{i1}+X_{i1}+r_iX_{i0}^3+2D_0D_1X_{i0}+2\mu_iD_0X_{i0}=0. \tag{3.14b}$$

Eq. (3.14a) can be solved as

$$X_0(T_0,T_1)=A_i(T_1)e^{jT_0}+B_ie^{jT_0}+c.c., \tag{3.15}$$

where $B_i=G_i/2(1-\omega^2)$.

Substituting Eq. (3.15) into Eq. (3.14b) leads to

$$\begin{aligned}D_0^2X_{i1}+X_{i1}=&-r_i[A_i^3e^{3jT_0}+3A_i^2B_ie^{j(2+\omega)T_0}+3A_iB_i^2e^{j(1+2\omega)T_0}\\ &+B_i^3e^{3j\omega T_0}+3\bar{A}_i^2B_ie^{j(\omega-2)T_0}+3A_iB_i^2e^{j(1-2\omega)T_0}]-[3r_iA_i^2\bar{A}_i+6r_iA_iB_i^2\\ &+2j\mu_iA_i+2jD_1A_i]e^{jT_0}-[6r_iA_i\bar{A}_iB_i+3r_iB_i^3+2j\mu_i\omega B_i]e^{j\omega T_0}+c.c..\end{aligned} \tag{3.16}$$

The secular terms of Eq. (3.16) are eliminated by setting

$$3r_iA_i^2\bar{A}_i+6r_iA_iB_i^2+2j\mu_iA_i+2jD_1A_i+3r_i\bar{A}_i^2B_ie^{j\sigma T_1}=0. \tag{3.17}$$

Substituting Eq. (3.7a) into Eq. (3.17) and separating the result into real and imaginary parts, one can obtain the differential equations of $a_i(T_1)$ and $\varphi_i(T_1)$,

$$D_1a_i=-\mu_ia_i-\frac{3r_iB_i}{4\omega_0}a_i^2\sin\varphi_i, \tag{3.18a}$$

$$D_1\varphi_i=\sigma-\frac{9r_i}{\omega_0}\left(B_i^2+\frac{a_i^2}{8}+\frac{B_i}{4}a_i\cos\varphi_i\right), \tag{3.18b}$$

where $\varphi_i=T_1\sigma-3\beta_i$.

By setting $D_1a_i=0$ and $D_1\varphi_i=0$, the equations for the amplitude $\bar{a}_i$ and the phase $\bar{\varphi}_i$ of the steady-state solutions of the 1/3 sub-harmonic resonance can be obtained as

$$-\mu_i\bar{a}_i-\frac{3r_iB_i}{4\omega_0}\bar{a}_i^2\sin\bar{\varphi}_i=0, \tag{3.19a}$$

$$\sigma-\frac{9r_i}{\omega_0}\left(B_i^2+\frac{\bar{a}_i^2}{8}+\frac{B_i}{4}\bar{a}_i\cos\bar{\varphi}_i\right)=0. \tag{3.19b}$$

Eliminating $\bar{\varphi}_i$ from Eq. (3.19), one can get the amplitude-frequency equation of the 1/3 sub-harmonic resonance for each span of the plate

$$\bar{a}_i^4+\left(12B_i^2-\frac{16\sigma}{9r_i}\right)\bar{a}_i^2+\frac{64}{81r_i^2}[9\mu_i^2+(\sigma-9r_iB_i^2)^2]=0,\quad (i=1,2). \tag{3.20}$$

Solving Eq. (3.20) for $\bar{a}_i^2$ yields

$$\bar{a}_i^2=P_i\pm\sqrt{P_i^2-Q_i}, \tag{3.21}$$

where

$$P_i=\frac{8\sigma}{9r_i}-6B_i^2\quad\text{and}\quad Q_i=\frac{64}{81r_i^2}[9\mu_i^2+(\sigma-9r_iB_i^2)^2].$$

In Eq. (3.21), $\bar{a}_i^2$ is real and positive if and only if

$$P_i>0,\quad P_i^2\geq Q_i, \tag{3.22}$$

which is the sufficient and necessary existence condition for the 1/3 sub-harmonic resonance.

To analyze the stability of the steady-state solution of the 1/3 sub-harmonic resonance, Eq. (3.18) is linearized at $(\bar{a}_i,\bar{\varphi}_i)$ about the perturbation variables Δa_i and $\Delta\varphi_i$,

$$D_1\Delta a_i=-\left(\mu_i+\frac{3r_iB_i\bar{a}_i}{2}\sin\bar{\varphi}_i\right)\Delta a_i-\frac{3r_iB_i\bar{a}_i^2}{4}\cos\bar{\varphi}_i\Delta\varphi_i, \tag{3.23a}$$

$$D_1\Delta\varphi_i=-\frac{9r_i}{4}(\bar{a}_i+B_i\cos\bar{\varphi}_i)\Delta a_i+\frac{9r_iB_i\bar{a}_i}{4}\sin\bar{\varphi}_i\Delta\varphi_i. \tag{3.23b}$$

According to Eq. (3.19), the characteristic equation of Eq. (3.23) can be expressed as

$$\begin{vmatrix} \lambda_i+\left(\mu_i+\dfrac{3r_iB_i\bar{a}_i}{2}\sin\bar{\varphi}_i\right) & \dfrac{3r_iB_i\bar{a}_i^2}{4}\cos\bar{\varphi}_i \\ \dfrac{9r_i}{4}(\bar{a}_i+B_i\cos\bar{\varphi}_i) & \lambda_i-\dfrac{9r_iB_i\bar{a}_i}{4}\sin\bar{\varphi}_i \end{vmatrix}$$
$$=\lambda_i^2+2\mu_i\lambda_i+\frac{3}{2}\left(\frac{3r_i\bar{a}_i}{4}\right)^2(\bar{a}_i^2-P_i)=0. \tag{3.24}$$

From the Routh-Hurwitz criterion [34], the steady-state vibration is asymptotically stable if and only if

$$\mu_i>0 \quad \text{and} \quad \frac{3}{2}\left(\frac{3r_i\bar{a}_i}{4}\right)^2(\bar{a}_i^2-P_i)>0.$$

4 Numerical results and discussions

4.1 Verification of the present analytical methodology

In order to validate the present methodology, comparisons are made between the present analytical solutions and the Runge-Kutta numerical integration method [35,36] in which Eqs. (3.1) and (3.13) are directly solved by the numerical integration method. In the calculations, the structural and material properties of the two-span composite laminated plate are: $E_{11}=7.6\times10^{10}\text{N/m}^2$, $E_{22}=5.6\times10^9\text{N/m}^2$, $G_{12}=2.3\times10^9\text{N/m}^2$, $v_{12}=0.21$, $v_{21}=0.0136$, $l=0.8\text{m}$, $h=0.0036\text{m}$ and $\rho=1460\text{kg/m}^3$. The ply angle of the composite laminated plate is $[\theta,-\theta,-\theta,\theta]$, where θ changes from 0° to 90°.

Figs. 2 and 3 show the amplitude-frequency curves at the center of each span of the plate for the primary resonance and 1/3 sub-harmonic resonance obtained by the present and the Runge-Kutta numerical integration methods. In these figures, the solid lines are corresponding to the asymptotically stable solutions and the dashed lines correspond to the unstable solutions. w represents the vibration amplitude at the center of each span of the plate.

From the observation of Figs. 2 and 3, it can be concluded that the present approximately analytical solutions coincide with the numerical integration results very well. Satisfactory precision can be acceptable for engineering applications. These results certify the correctness of the approximately analytical solutions in this paper and can present satisfactory precision.

4.2 Primary resonance

When the internal line support is placed at the symmetric location of the plate, i.e., $l_1=l_2$, this plate is ordered two-span structure. However, the internal line support may usually be displaced from the symmetric location for some reasons such as manufacturing tolerances which turn the ordered periodic structures into disordered ones. In this work,

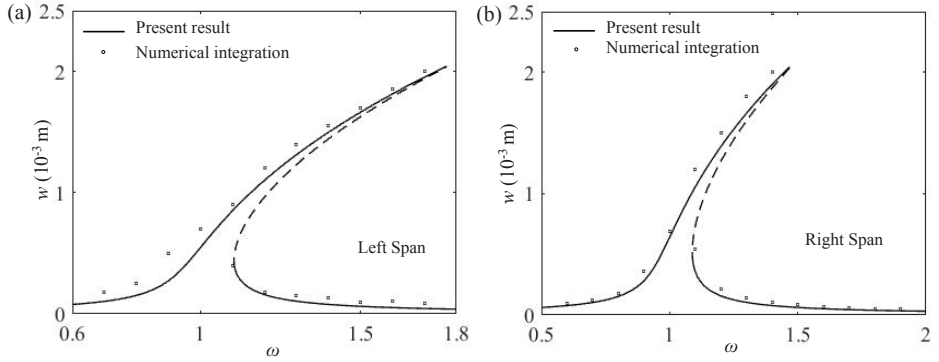

Figure 2: Comparison of the amplitude-frequency curves of primary resonance calculated by the present method with those by numerical integration method when $v=0.05$, $\theta=45^\circ$.

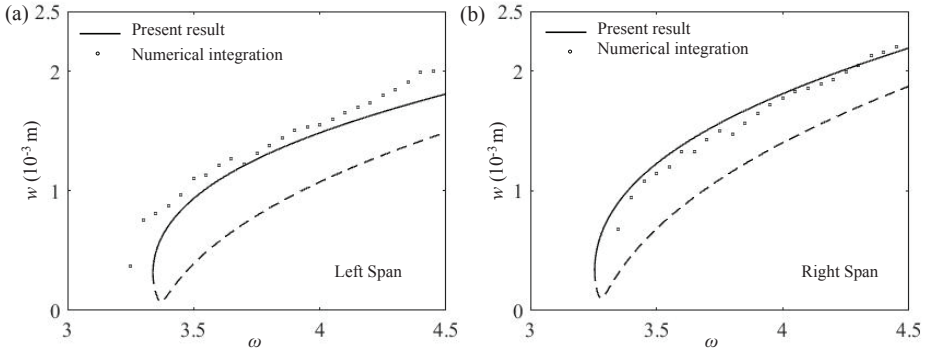

Figure 3: Comparison of the amplitude-frequency curves of 1/3 sub-harmonic resonance calculated by the present method with those by numerical integration method when $v=0.05$, $\theta=45^\circ$.

the disorder ratio v is firstly taken into consideration on the nonlinear resonance of the two-span composite laminated plate. Here, $v=0$ denotes the ordered two-span structure and $v\neq 0$ denotes the disordered one.

Figs. 4 and 5 display the effect of disorder ratio on the amplitude-frequency curves of primary resonance when ply angle θ is a constant. Fig. 4(a) is the ordered case and it can be seen that the amplitude-frequency curves of left and right span totally coincide with each other. This means that the vibration responses of the same symmetric points on both spans are total the same, including the same primary resonance frequencies and vibration amplitudes. Figs. 4(b)-(d) show the amplitude-frequency curves of disordered cases. It is observed that the resonance frequency of the right span is lower than that of the left span, that is to say, the primary resonance phenomenon can occur in the right span in relatively lower frequency than that in the left span. And the response amplitude of the right span is bigger than that of the left span at the same excitation frequency before resonance, which illustrates that the right span of the plate plays a leading role in

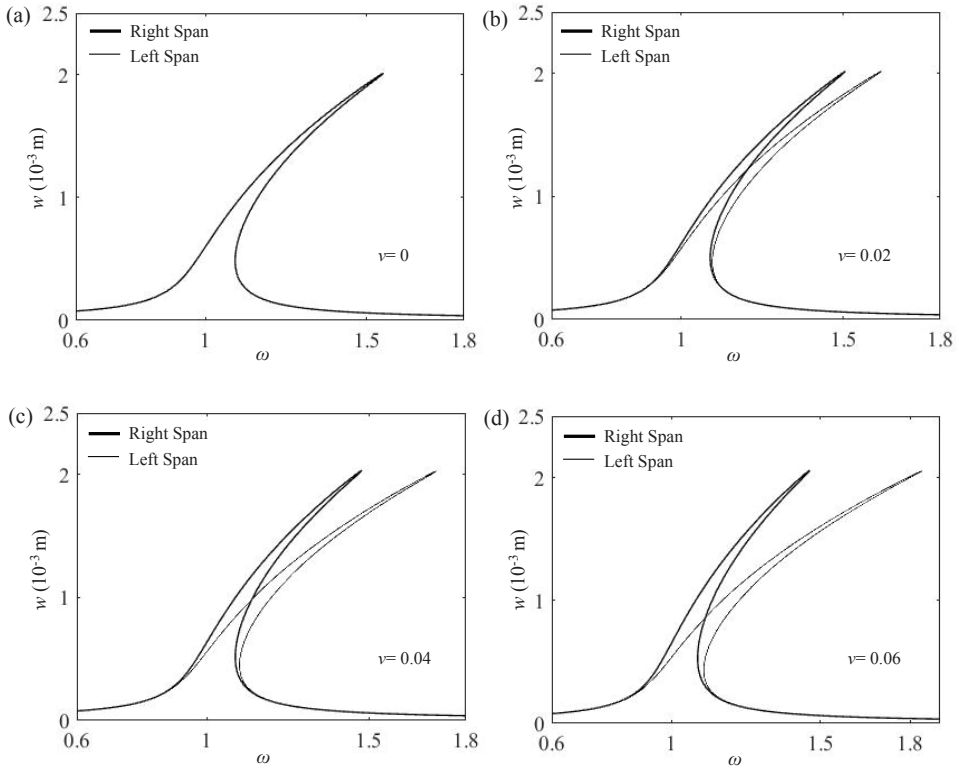

Figure 4: Amplitude-frequency curves of primary resonance varying with disorder ratio v when $\theta=45^\circ$.

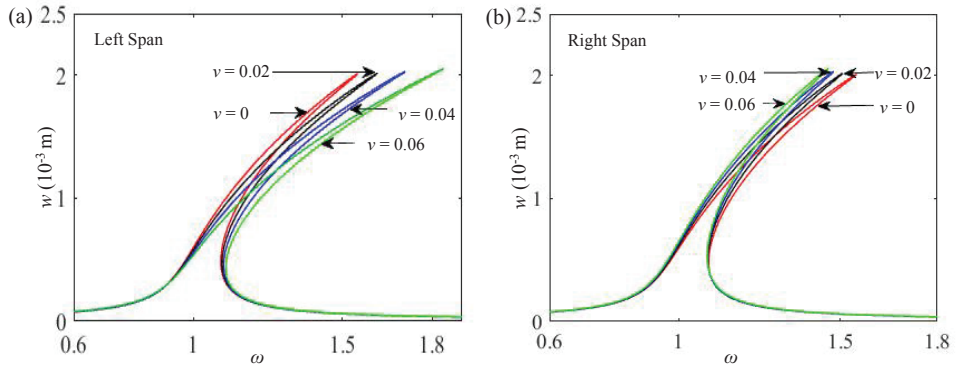

Figure 5: Amplitude-frequency curves of primary resonance on each span of the plate varying with disorder ratio v when $\theta=45^\circ$.

the primary resonance. These disparities become more obvious with the disorder ratio increasing. This is the so called vibration localization phenomenon.

Fig. 5 illustrates that the vibration amplitude gradually decreases and the resonance

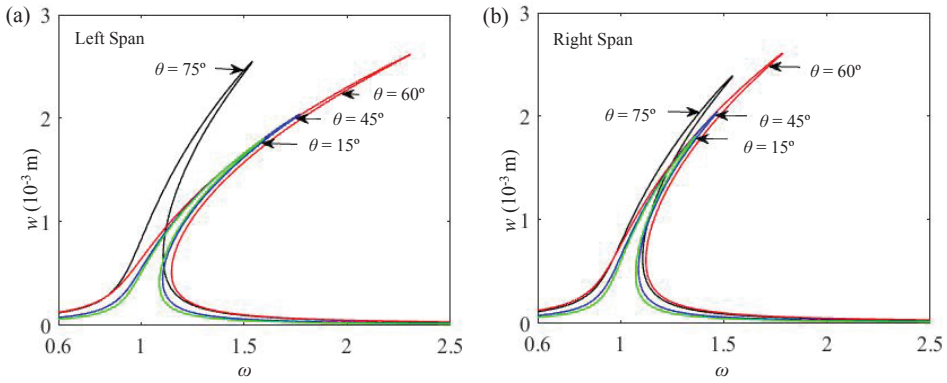

Figure 6: Amplitude-frequency curves of primary resonance on each span of the plate varying with ply angle θ when $v=0.05$.

frequency gradually increases with the increase of the disorder ratio at the same excitation frequency for the left span when the ply angle is a constant. Oppositely, the vibration amplitude gradually increases and the resonance frequency gradually decreases with the disorder ratio increasing at the same excitation frequency for the right span.

Fig. 6 displays the effect of different ply angles on the amplitude-frequency curves of primary resonance when disorder ratio is constant. It can be observed that the vibration amplitude is minimal at the same excitation frequency and resonance frequency is maximal when ply angle $\theta=60^\circ$ for both the left and right spans of the plate.

4.3 1/3 Sub-harmonic resonance

Figs. 7 and 8 show the effects of different disorder ratios on the amplitude-frequency curves of 1/3 sub-harmonic resonance when ply angle θ is constant. The solid lines are for the asymptotically stable solutions and the dashed lines are for the unstable ones. It is observed from Fig. 7(a) that the left and right spans of the plate have totally the same amplitude-frequency curves for the ordered two-span composite laminated plate, including the length of interval of the frequency and vibration amplitude. Figs. 7(b)-(d) correspond to the disordered cases. From these figures, it can be seen that the intervals of resonance frequency for the right span plate are bigger than those for the left span plate, and also the response amplitudes of the right span are bigger than those of the left one at the same excitation frequency, which illustrates that the right span plate plays a leading role in the 1/3 sub-harmonic resonance. Furthermore, these differences of vibration amplitudes and resonance intervals between the right and left spans become more obvious with the disorder ratio increasing. So, it can be concluded that with the increase of the disorder ratio, the nonlinear vibration localization degree will be strengthened.

From Fig. 8, it can be observed that the vibration amplitude and length of interval of resonance frequency gradually decrease with the increase of the disorder ratio for the

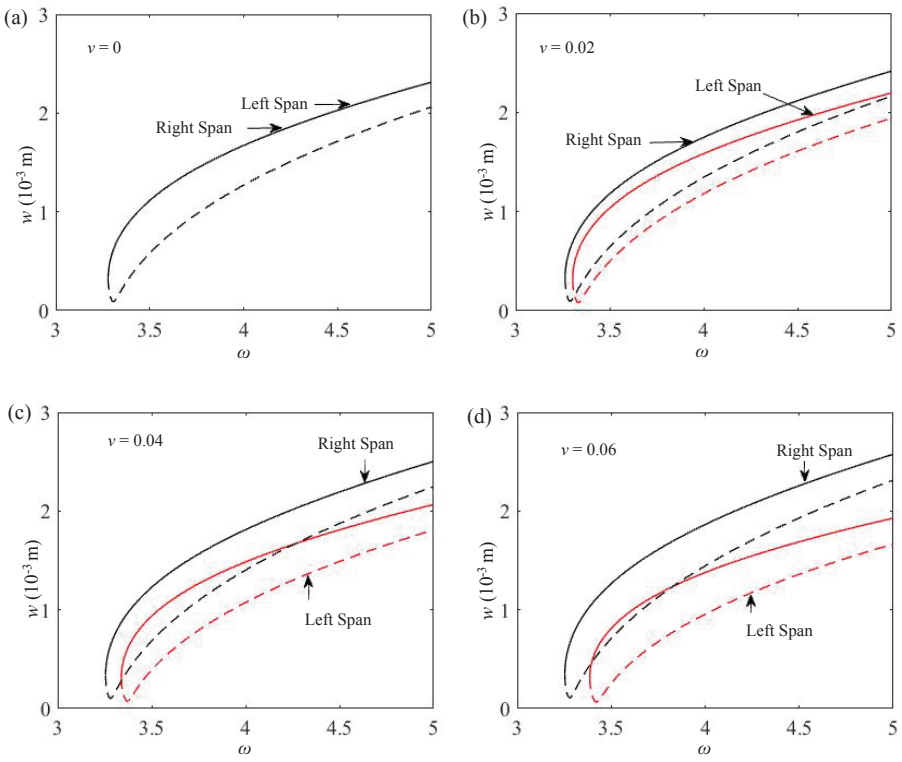

Figure 7: Amplitude-frequency curves of 1/3 sub-harmonic resonance varying with disorder ratio v when ply angle $\theta=45^\circ$.

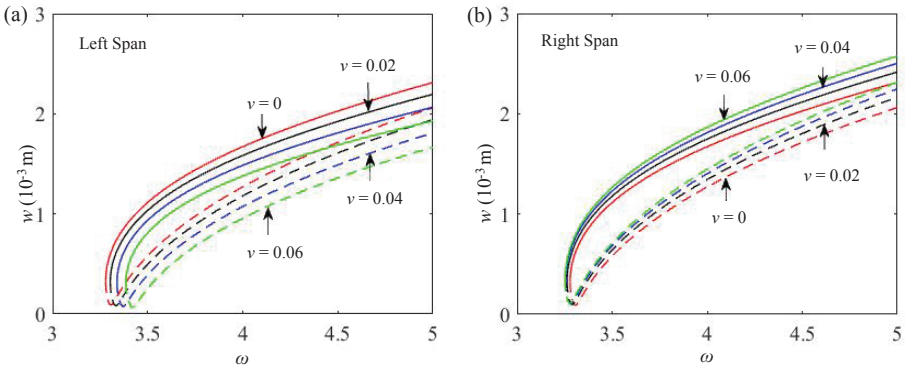

Figure 8: Amplitude-frequency curves of 1/3 sub-harmonic resonance on each span of the plate varying with disorder ratio v when ply angle $\theta=45^\circ$.

left span plate when $\theta=45^\circ$. Oppositely, the vibration amplitude and length of interval of resonance frequency gradually increase with the disorder ratio increasing for the right span.

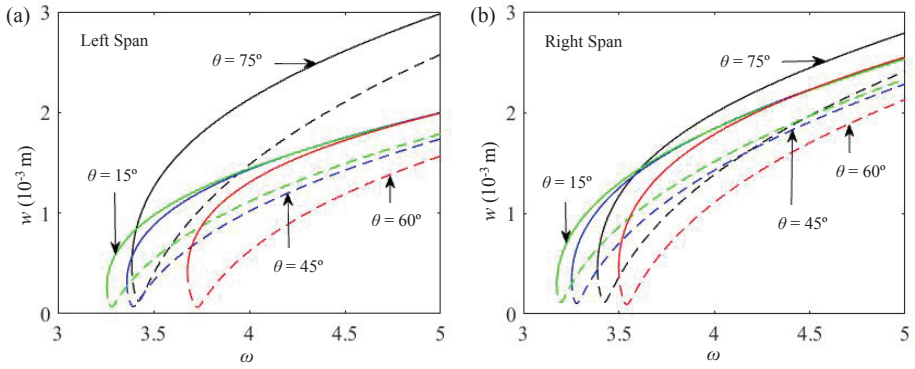

Figure 9: Amplitude-frequency curves of 1/3 sub-harmonic resonance on each span of the plate varying with ply angle θ when $v=0.05$.

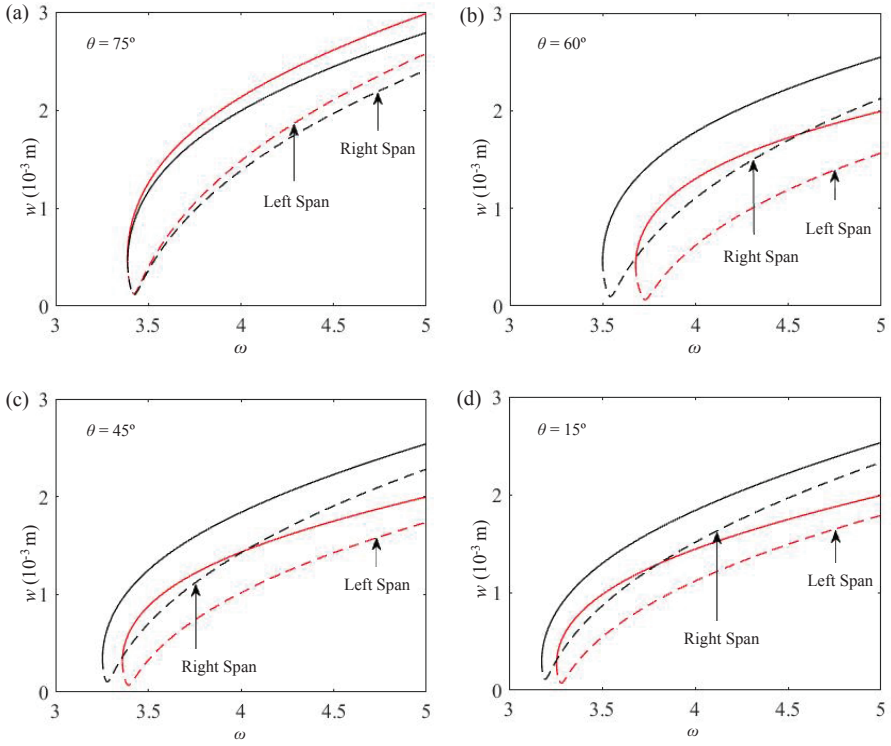

Figure 10: Amplitude-frequency curves of 1/3 sub-harmonic resonance varying with ply angle θ when $v=0.05$.

Figs. 9 and 10 illustrate the influences of ply angle on 1/3 sub-harmonic resonance curves for a certain disorder ratio. From Fig. 9, it can be seen that the vibration amplitude is minimal at the same excitation frequency and the length of interval of the frequency is also minimal when ply angle θ is 60° for both the left and right spans of the plate. From

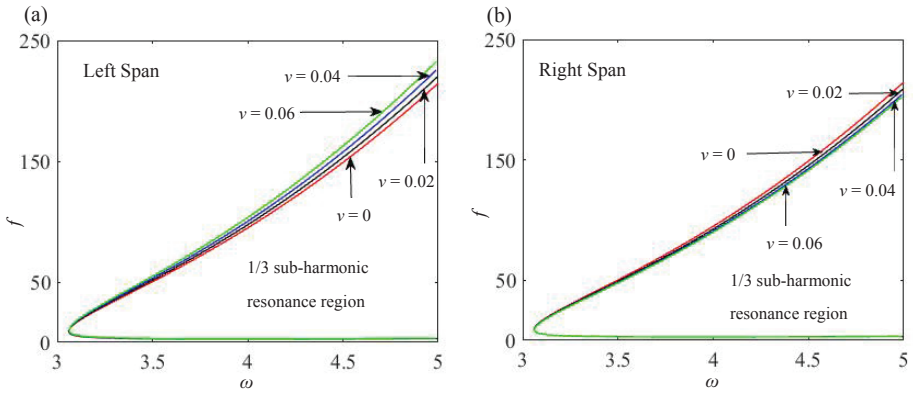

Figure 11: Regions for 1/3 sub-harmonic resonance on each span of the plate varying with disorder ratio v when ply angle $\theta=45^\circ$.

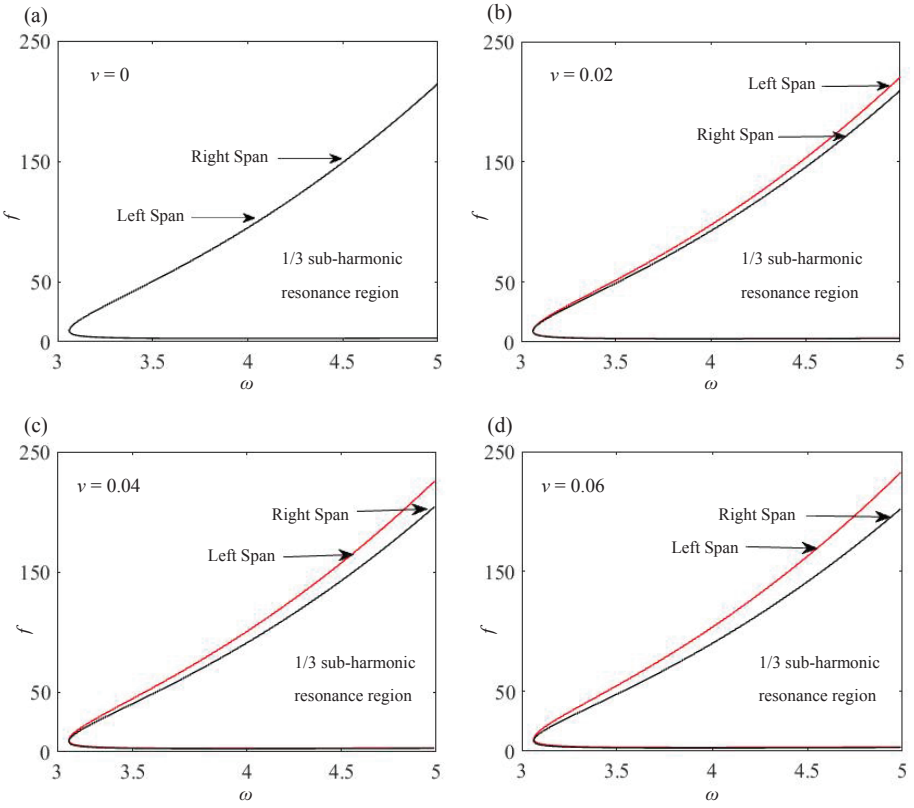

Figure 12: Regions for 1/3 sub-harmonic resonance with different v when $\theta=45^\circ$.

Fig. 10, it is observed that the response amplitude of the right span is bigger than that of the left span at the same excitation frequency when ply angle θ is 60°, 45° and 15°, but

the contrary case happens when ply angle θ is increased to 75°.

Figs. 11 and 12 display the effect of disorder ratio on the existence regions for $1/3$ sub-harmonic resonance on each span of the plate. From Fig. 11, it can be found that the regions for $1/3$ sub-harmonic resonance change slightly for different disorder ratios for each span plate. With the increase of the disorder ratio, the excitation amplitude f for $1/3$ sub-harmonic resonance becomes a little large for the left span and a little small for the right span plate.

Fig. 12(a) shows that the left and right spans of the plate have exactly the same existence regions for $1/3$ sub-harmonic resonance for the ordered two-span plate. Figs. 12(b)-(d) represent the disordered cases and from these figures it can be observed that the intervals of the frequency ratio for $1/3$ sub-harmonic resonance are almost equal for both the left and right spans, but the ranges for $1/3$ sub-harmonic resonance of the left span are wider than those of the right span. And the larger the disorder degree is, the more different the ranges for $1/3$ sub-harmonic resonance between the left and right spans become.

5 Conclusions

The nonlinear primary resonance and $1/3$ sub-harmonic resonance of ordered and disordered 2D two-span composite laminated plates are investigated. The equation of motion of the structure is established applying Hamilton's principle considering the geometrical nonlinearity, and is transformed into ordinary differential equation by Galerkin's method. The method of multiple scales is used to obtain the amplitude-frequency relations of the primary and $1/3$ sub-harmonic resonances. The effects of the disorder ratio and ply angle on the nonlinear resonances and vibration localization phenomenon are analyzed. The comparisons of the present analytical solutions with those of the numerical integration are made to verify the correctness and satisfactory precision of the present results. From the investigation, the following conclusions can be drawn:

(1) For the ordered two-span composite laminated plate, the amplitude-frequency curves for both the primary resonance and the $1/3$ sub-harmonic resonance of the two spans of the plate are totally the same. And the existence regions for $1/3$ sub-harmonic resonance of the two spans totally coincide with each other.

(2) The nonlinear vibration localization phenomenon occurs for the disordered two-span plate. The differences of the vibration amplitude and resonance frequency between the left and right span plate become more obvious with the increase of the disorder ratio, i.e., the larger the disorder degree is, the stronger the nonlinear vibration localization property becomes.

(3) The ply angle is a very influential factor on the nonlinear vibration behaviors including the primary and the sub-harmonic resonances.

Nomenclature

l,l_1,l_2,h	=	total length, left span length, right span length, uniform thickness of the two-span plate
E_{11},E_{22},G_{12}	=	elastic and shear moduli
ρ	=	plate density
v_{12},v_{21}	=	Poisson's ratio
Δl	=	displacement of the internal line support to the symmetric location of the plate
$T_i,U_i,\delta W_i$	=	strain energy, kinetic energy, virtual work
v	=	disorder ratio
c	=	structural damping coefficient
n	=	number of layers
σ	=	detuning parameter
θ	=	ply angle of the composite laminated plate
ε	=	small parameter
N	=	in-plane compression force
D_0,D_1	=	$d(\ )/dT_0$, $d(\ )/dT_1$
$F\cos(\Omega t)$	=	uniform harmonic external excitation
D_0^2	=	$d^2(\ )/dT_0^2$
w_1,w_2	=	transverse displacement of left, right span plate
$\overline{\omega}$	=	structural natural frequency
$W_i(x_i),Q_i(t)$	=	mode shape, generalized coordinate
ω	=	dimensionless external excitation frequency
$Q_{11},Q_{12},Q_{22},Q_{66}$	=	stiffness coefficients

Acknowledgments

This research is supported by the National Natural Science Foundation of China (Nos. 11572007 and 11172084).

References

[1] A. S. VELETSOS AND N. M. NEWMARK, *Determination of natural frequencies of continuous plates hinged along two opposite edges*, ASME J. Appl. Mech., 23 (1956), pp. 97–102.
[2] H. ABRAMOVICH, M. EISENBERGER AND O. SHULEPOV, *Vibration of multi-span non-symmetric composite beams*, Composites Eng., 5(4) (1995), pp. 397–404.
[3] R. T. WANG AND T. Y. LIN, *Vibration of multispan Mindlin plates to a moving load*, J. Chinese Institute Eng., 19(4) (1996), pp. 467–477.
[4] R. T. WANG, *Vibration of multi-span Timoshenko beams to a moving force*, J. Sound Vib., 207(5) (1997), pp. 731–742.

[5] Y. XIANG AND G. W. WEI, *Exact solution for vibration of multi-span rectangular Mindlin plates*, J. Vib. Acoustics, 124 (2002), pp. 545–551.
[6] Y. B. ZHAO, G. W. WEI AND Y. XIANG, *Plate vibration under irregular internal supports*, Int. J. Solids Struct., 39 (2001), pp. 1361–1383.
[7] Y. XIANG, Y. B. ZHAO AND G. W. WEI, *Levy solutions for vibration of multi-span rectangular plates*, Int, J. Mech. Sci., 44 (2002). pp. 1195–1218.
[8] Y. XIANG AND J. N. REDDY, *Natural vibration of rectangular plates with an internal line hinge using the first order shear deformation plate theory*, J. Sound Vib., 263 (2003), pp. 285–297.
[9] C. F. LV, Y. Y. LEE, C. W. LIM AND W. Q. CHEN, *Free vibration of long-span continuous rectangular Kirchhoff plates with internal rigid line supports*, J. Sound Vib., 297 (2006), pp. 351–364.
[10] Y. MIKATA, *Orthogonality condition for a multi-span beam, and its application to transient vibration of a two-span beam*, J. Sound Vib., 314 (2008), pp. 851–866.
[11] Z. G. SONG AND F. M. LI, *Vibration and aeroelastic properties of ordered and disordered two-span panels in supersonic airflow*, Int. J. Mech. Sci., 81 (2014), pp. 65–72.
[12] F. M. LI AND Z. G. SONG, *Vibration analysis and active control of nearly periodic two-span beams with piezoelectric actuator/sensor pairs*, Appl. Math. Mech., 36(3) (2015), pp. 279–292.
[13] E. ÖZKAYA, S. M. BAGATLI AND H. R. ÖZ, *Non-linear transverse vibrations and 3:1 internal resonance of a beam on multiple supports*, J. Vib. Acoustics, 130(2) (2008), pp. 1–11.
[14] S. M. BAGATLI, H. R. ÖZ AND E. ÖZKAYA, *Non-linear transverse vibrations and 3:1 internal resonance of a tensioned beam on multiple supports*, Math. Comput. Appl., 16(1) (2011), pp. 203–215.
[15] S. DAVTABAL, K. C. WOO, C. P. PAGWIWOKO AND S. LENCI, *Nonlinear vibration of a multi-span continuous beam subject to periodic impact excitation*, Meccanica, 50 (2015), pp. 1227–1237.
[16] R. LEWANDOWSKI, *Nonlinear free vibrations of multispan beams on elastic supports*, Comput. Structures, 32(2) (1989), pp. 305–312.
[17] S. A. EFTEKHARI AND A. A. JAFARI, *A mixed method for forced vibration of multi-span rectangular plates carrying moving masses*, Arab J. Sci. Eng., 2 39 (2014), pp. 3225–3250.
[18] E. TUBALDI, F. ALIJANI AND M. AMABILI, *Non-linear vibrations and stability of a periodically supported rectangular plate in axial flow*, Int. J. Nonlinear Mech., 66 (2014), pp. 54–65.
[19] E. TUBALDI AND M. AMABILI, *Vibrations and stability of a periodically supported rectangular plate immersed in axial flow*, J. Fluids Structures, 39 (2013), pp. 391–407.
[20] Y. SHEN, S. YANG, H. XING AND H. MA, *Primary resonance of Duffing oscillator with two kinds of fractional-order derivatives*, Int. J. Nonlinear Mech., 47 (2012), pp. 975–983.
[21] Y. J. SHEN, S. F. WEN, X. H. LI, S. P. YANG AND H. J. XING, *Dynamical analysis of fractional-order nonlinear oscillator by incremental harmonic balance method,* Nonlinear Dyn., 85 (2016), pp. 1457–1467.
[22] Y. J. SHEN, S. P. YANG, H. J. XING AND G. S. GAO, *Primary resonance of Duffing oscillator with fractional-order derivative*, Commun. Nonlinear Sci. Numer. Simulation, 17 (2012), pp. 3092–3100.
[23] M. ROSTAMI AND M. HAERI, *Undamped oscillations in fractional-order Duffing oscillator*, Signal Processing, 107 (2015), pp. 361–367.
[24] X. GAO AND J. B. YU, *Chaos in the fractional order periodically forced complex Duffing's oscillators*, Chaos, Solitons and Fractals, 24 (2005), pp. 1097–1104.
[25] Z. M. GE AND C. Y. OU, *Chaos in a fractional order modified Duffing system*, Chaos, Solitons and Fractals, 34 (2007), pp. 262–291.
[26] F. M. LI AND G. YAO, *1/3 Subharmonic resonance of a nonlinear composite laminated cylindrical shell in subsonic air flow*, Composite Structures, 100 (2013), pp. 249–256.

[27] H. M. ABDELHAFEZ, *Resonance of multiple frequency excitated systems with quadratic, cubic and quartic non-linearity*, Math. Comput. Simulation, 61 (2002), pp. 17–34.
[28] D. YOUNESIAN AND H. NOROUZI, *Frequency analysis of the nonlinear viscoelastic plates subjected to subsonic flow and external loads*, Thin-Walled Structures, 92 (2015), pp. 65–75.
[29] F. ALIJANLI AND M. AMABILI, *Nonlinear vibrations of laminated and sandwich rectangular plates with free edges: Part 1: Theory and numerical simulations*, Composite Structures, 105 (2013), pp. 422–436.
[30] F. ALIJANLI, M. AMABILI, G. FERRARI AND V. D'ALESSANDRO, *Nonlinear vibrations of laminated and sandwich rectangular plates with free edges: Part 2: Experiments and comparisons*, Composite Structures, 105 (2013), pp. 437–445.
[31] I. D. BRESLAVSKY, M. AMABILI AND M. LEGRAND, *Physically and geometrically non-linear vibrations of thin rectangular plates*, Int. J. Nonlinear Mech., 58 (2014), pp. 30–40.
[32] J. N. REDDY, Mechanics of Laminated Composites Plates and Shells: Theory and Analysis, 2nd ed. Boca Raton (FL), CRC Press, 2004.
[33] A. HOUMAT, *Nonlinear free vibration of laminated composite rectangular plates with curvilinear fibers*, Composite Structures, 106 (2013), pp. 211–224.
[34] H. Y. HU, E. H. DOWELL AND L. N. VIRGIN, *Resonance of a harmonically forced Duffing oscillator with time delay state feedback*, Nonlinear Dyn., 15(4) (1998), pp. 311–327.
[35] R. CAPONETTO, G. DONGOLA, L. FORTUNA AND I. PETRAS, Fractional-order System and Control: Fundationals and Applications, Springer-Verlag, London, 2010.
[36] F. M. LI, G. YAO AND Y. ZHANG, *Active control of nonlinear forced vibration in a flexible beam using piezoelectric material*, Mech. Adv. Materials Structures, 23(3) (2016), pp. 311–317.